a flat frequency characteristic and its level approximately gives the phase noise level, $S_{\Phi, NL}(0)$. Thus, we can estimate the magnitude of fibre-nonlinearity-induced phase noise by measuring the flat component level; note that the 3 dB linewidth does not allow the phase noise to be quantified. As $P_{\Phi, NL}$ increases, the broadband component predominates in the field spectrum while the initial carrier-like component decreases. If $P_{\Phi, NL} \gg 1$, the bandwidth of the broadband component increases linearly with $P_{\Phi, NL}$ (see eqn. 9), and becomes much wider than that of the ASE noise.

Effect on transmission systems: Carrier spectral deformation due to the fibre-nonlinearity-induced phase noise results in signal power degradation when the signal passes through a filter in a receiver. A coherent detection system, which uses an electrical filter in its intermediate-frequency (IF) stage, suffers from this power degradation, as well as signal decision error due to phase fluctuation [3]. Even a direct-detection system, which uses an optical filter to reduce spontaneous-spontaneous beat noise, is affected by the phase noise, though it is generally recognised to be insensitive to phase.

Fig. 2 shows the signal power degradation, which is defined as the ratio of the filter output signal power to the input power, as a function of the phase noise power, $P_{\Phi, NL}$. In this calculation, the ASE noise bandwidth $\Delta\omega_{opt}$ is 125 GHz. Filters are assumed to have Lorentzian (1st Butterworth) characteristics. The IF filter bandwidth is 5 GHz for a 2·5 Gbit/s heterodyne receiver, and the optical filter bandwidth is 125 GHz or 375 GHz for a direct detection receiver.

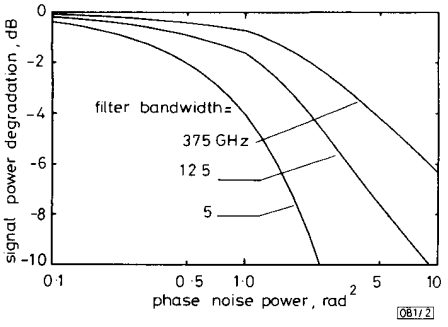

Fig. 2 *Signal power degradation against phase noise power*

In coherent detection systems, a $P_{\Phi, NL}$ value of 0·25 results in a 1 dB degradation in signal power. This phase noise level corresponds to a phase error variance (phase noise power in the signal band) of 0·01. In DPSK systems, this variance yields an error rate of 10^{-9}. Thus, the signal power degradation is as significant as the signal decision error due to phase fluctuation. In direct-detection systems, $P_{\Phi, NL}$ values of 0·54 and 1·4 give rise to a 1 dB power degradation for optical filter bandwidths of 125 and 375 GHz, respectively. Although less affected by the power degradation than coherent detection, the performance of a direct detection system should be estimated while taking the degradation into account. This degradation can become one of the factors limiting the transmission length of systems employing optical amplifiers to compensate for fibre losses because the phase noise rapidly increases with the number of amplifiers [3]. We can estimate the allowable length of such systems by considering that the resulting field spectrum is affected by the optical filters located in the amplifiers.

Conclusions: An approximate analytical expression was presented for the spectral lineshape of the optical carrier wave corrupted by fibre-nonlinearity-induced phase noise. It was shown that the phase noise causes lineshape deformation with both tails significantly enhanced over hundreds of gigahertz. This deformation affects the performance of both coherent and direct detection systems because the signal power degrades significantly when the signal passes through the receiver's filter.

Acknowledgment: The authors wish to thank H. Ishio and T. Ito for their encouragement.

17th August 1992

M. Murakami and S. Saito (*NTT Transmission Systems Laboratories, 1-2356, Take, Yokosuka-shi, Kanagawa 238-03, Japan*)

References

1 MARCUSE, D.: 'Effect of fiber nonlinearity on long distance transmission', *J. Lightwave Technol.*, 1991, **LT-9**, pp. 121–128
2 SAITO, S., MURAKAMI, M., NAKA, A., FUKADA, Y., IMAI, T., AIKI, M., and ITO, T.: '2·5 Gbit/s, 80–100 km spaced in-line amplifier transmission experiment over 2,500–4,500 km'. IOOC/ECOC'91, Paris, A. PDP.5, 1991
3 GORDON, J. P., and MOLLENAUER, L. F.: 'Phase noise in photonic communications systems using linear amplifiers', *Opt. Lett.*, 1991, **15**, pp. 1351–1353
4 RYU, S.: 'Signal linewidth broadening due to fiber nonlinearities in long-haul transmission systems', *Electron. Lett.*, 1991, **27**, pp. 1527–1529

MODULATION BANDWIDTH ENHANCEMENT IN SINGLE QUANTUM WELL GaAs/AlGaAs LASERS

T. R. Chen, B. Zhao, Y. Yamada, Y. H. Zhuang and A. Yariv

Indexing terms: Semiconductor lasers, Lasers

The state filling effect in semiconductor quantum well lasers significantly affects the modulation dynamics. The state filling effect strongly depends on the optical confining layer structure. As a direct consequence of the reduction of the state filling effect in a properly designed graded index separate confinement heterostructure, a record 3 dB bandwidth in excess of 9 GHz has been obtained in uniformly pumped single quantum well GaAs/AlGaAs lasers by a careful tailoring of the device parameters.

The state filling effect has been proposed as a major source [1, 2] responsible for the degradation of the modulation bandwidth of quantum well (QW) lasers compared to the expected value previously calculated [3, 4]. In the previous gain calculations, only the carrier population in the quantised energy states of the QW was considered. The carrier population in the energy states in the separate confinement heterostructure (SCH) were omitted. It was this omission which causes an overestimation of the differential gain enhancement in the QW structure. An incorporation of the carrier population in the optical confining region into the gain evaluation results in a substantial reduction of the differential gain in QW lasers [2]. The state filling effect is, in principle, inherent in any QW structure due to the Fermi distribution of the injected carriers. Other mechanisms have also been proposed to explain the variation of high speed performance of QW lasers which are associated with an injected carrier transport process [5] and well barrier hole burning [6]. The theoretical analysis accounting for the state filling effect indicates that the differential gain depends strongly on the optical confining structure of the SCH QW structure. By proper design of the SCH configuration, the degraded differential gain can be restored to a certain extent. For a different SCH structure, it has been shown experimentally that the differential gain can vary by a factor of 3 [7]. In this paper, we report the high speed modulation performance of a new design of the SCH structure [7], which results in a record modulation bandwidth of 9 GHz for single quantum well (SQW) GaAs/AlGaAs lasers.

The new design of the graded index separate confinement heterostructure (GRINSCH) employs, as shown in Fig. 1, an Al mole fraction from $x = 0·3$ to 0·5 instead of the commonly used value of $x = 0·2$ to 0·5 [8, 9]. As a result, the energy

difference between the first quantised state in the well and the lowest energy state in the GRINSCH region increases. This results in a differential gain increase due to the reduction of the state filling effect [2]. The fabrication of the SQW device involves a two step crystal growth. In the first step, a GRINSCH SQW GaAs/AlGaAs laser structure was grown on an *n*-GaAs substrate by a molecular beam epitaxy technique. The width of the GaAs SQW is 100 Å which is sandwiched between a pair of GRINSCH layers. The thickness of the GRINSCH layer is 2000 Å. The broad area lasers showed a threshold current density of 320 A/cm^2 at a cavity length of 900 μm. In the second step, a buried heterostructure (BH) was regrown by a liquid phase epitaxy technique. The width of the active stripe was 4 μm. The wafer was processed into BH lasers (as schematically shown in Fig. 1) by a standard fabrication technique and mounted junction up on high speed mounts for direct current modulation. To reduce the parasitic capacitance a narrow mesa of 8–10 μm was etched into the wafer around the active stripe.

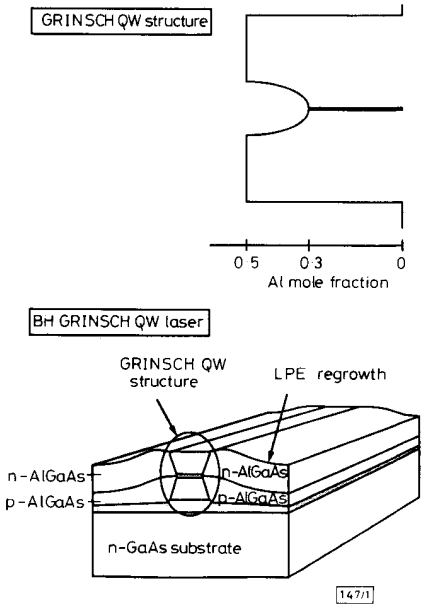

Fig. 1 *Schematic structure of GaAs/AlGaAs single quantum well buried heterostructure lasers*

Owing to the presence of the damping we cannot increase the modulation bandwidth unlimitedly by only increasing the photon density within the laser cavity. For a laser with given device parameters, there exists a maximum modulation bandwidth at a certain photon density [10]. Both this maximum modulation bandwidth and corresponding photon density depend on the laser device parameters. The restoration of a higher value of differential gain in the present designed SQW lasers gives the potential of an improved high speed performance. To actually achieve higher speed, a careful tailoring of the laser device parameters such as cavity length and mirror reflectivities is required.

For a laser with cavity length $L = 300\,\mu$m and cleaved mirrors (i.e. $R_1 = R_2 = 0{\cdot}3$), a maximum modulation bandwidth of 5·6 GHz is obtained. The threshold current of this laser is 10 mA and the lasing wavelength is $\sim 0{\cdot}85\,\mu$m. For an uncoated 150 μm long laser with threshold current of 16 mA, the maximum modulation bandwidth was ~6·2 GHz. However, when the reflectivity of one mirror was increased to 0·7 by a dielectric coating, a maximum modulation bandwidth in excess of 9 GHz was demonstrated as shown in Fig. 2. A further increase of the mirror reflectivity to 0·9 resulted in a decrease of the maximum modulation bandwidth to ~7·5 GHz. It is therefore concluded that for the GaAs SQW laser a cavity length of 150 μm with mirror reflectivities of 0·3 and 0·7 is a good (if not the best) combination for high speed operation. The maximum modulation bandwidth against threshold current for the SQW lasers is plotted in Fig. 3 to show the device parameter optimisation procedure.

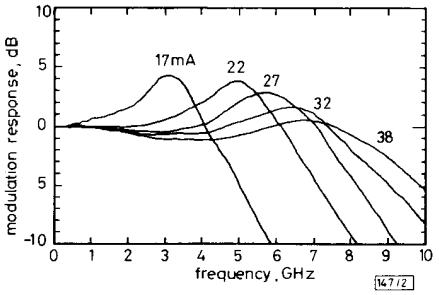

Fig. 2 *Modulation response of GaAs/AlGaAs SQW BH laser with cavity length of 150 μm and facet reflectivities $R_1 = 0{\cdot}3$, $R_2 = 0{\cdot}7$*

In conclusion, as a direct consequence of the reduction of the state filling effect in a specially designed graded index separate confinement heterostructure, a record 3 dB bandwidth in excess of 9 GHz has been obtained in uniformly pumped single quantum well GaAs/AlGaAs lasers by a careful tailoring of the device parameters. The idea can now be extended to other structures and material systems, such as MQW and strained layer QW lasers.

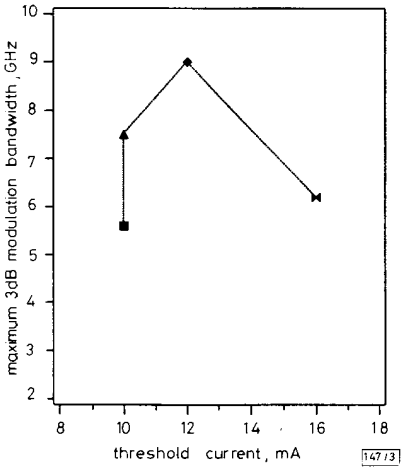

Fig. 3 *Maximum modulation bandwidth and threshold current for different lasers*

- ■ $L = 300\,\mu$m, $R_1 = R_2 = 0{\cdot}3$
- ▲ $L = 150\,\mu$m, $R_1 = 0{\cdot}3$, $R_2 = 0{\cdot}9$
- ● $L = 150\,\mu$m, $R_1 = 0{\cdot}3$, $R_2 = 0{\cdot}7$
- ⋈ $L = 150\,\mu$m, $R_1 = R_2 = 0{\cdot}3$

Acknowledgments: This work was supported by the Office of Naval Research, the Defense Advanced Research Project Agency and Air Force Office of Scientific Research.

24th August 1992

T. R. Chen, B. Zhao, Y. Yamada, Y. H. Zhuang and A. Yariv (*TJ Watson Sr. Laboratories of Applied Physics, 128-95, California Institute of Technology, Pasadena, California 91125, USA*)

References

1 ZHAO, B., CHEN, T. R., and YARIV, A.: 'Comparison of differential gain in single quantum well and bulk double heterostructure lasers', *Electron. Lett.*, 1991, **27**, pp. 2343–2344

2 ZHAO, B., CHEN, T. R., and YARIV, A.: 'Effect of state filling on the modulation response and the threshold current of quantum well lasers', *Appl. Phys. Lett.*, 1992, **60**, pp. 1930–1932

3 ARAKAWA, Y., VAHALA, K., and YARIV, A.: 'Quantum noise and dynamics in quantum well and quantum wire lasers', *Appl. Phys. Lett.*, 1984, **45**, pp. 950–952
4 SUEMUNE, I., COLDREN, L. A., YAMANISHI, M., and KAN, Y.: 'Extremely wide modulation bandwidth in a low threshold current strained quantum well laser', *Appl. Phys. Lett.*, 1988, **53**, pp. 1378–1380
5 NAGARAJAN, R., FUKUSHIMA, T., CORZINE, S. W., and BOWERS, J. E.: 'Effects of carrier transport on high-speed quantum well lasers', *Appl. Phys. Lett.*, 1991, **59**, pp. 1835–1837
6 RIDEOUT, W., SHARFIN, W. F., KOTELES, E. S., VASSELL, M. O., and ELMAN, B.: 'Well-barrier hole burning in quantum well lasers', *IEEE Photonics Technol. Lett.*, 1991, **3**, pp. 784–786
7 ZHAO, B., CHEN, T. R., YAMADA, Y., ZHUANG, Y. H., KUZE, N., and YARIV, A.: 'Evidence for state filling effect on high speed modulation dynamics of quantum well lasers', *Appl. Phys. Lett.*, 1992, **61**
8 DERRY, P. L., YARIV, A., LAU, K., BAR-CHAIM, N., LEE, K., and ROSENBERG, J.: 'Ultralow-threshold graded-index separate-confinement single quantum well buried heterostructure (Al, Ga)As lasers with high reflectivity coatings', *Appl. Phys. Lett.*, 1987, **50**, pp. 1773–1775
9 DERRY, P. L., CHEN, T. R., ZHUANG, Y. H., PASLASKI, J., MITTELSTEIN, M., VAHALA, K., and YARIV, A.: 'Spectral and dynamic characteristics of buried-heterostructure single quantum well (Al,Ga)As lasers', *Appl. Phys. Lett.*, 1988, **50**, pp. 271–273
10 ZHAO, B., CHEN, T. R., and YARIV, A.: 'On the high speed modulation bandwidth of quantum well lasers', *Appl. Phys. Lett.*, 1992, **60**, pp. 313–315

INTERNAL QUANTUM EFFICIENCY OF LASER DIODES

P. R. Claisse and G. W. Taylor

Indexing terms: Lasers, Semiconductor lasers

The internal quantum efficiency of laser diodes is determined from a consideration of current flow at threshold, and the corresponding quasi-Fermi level separation is used to evaluate the magnitude of all current components. The internal quantum efficiency is shown to be a strong function of temperature and cavity length. The results for single, multiple and strained quantum well structures are compared.

Internal quantum efficiency is one of the key parameters describing the operating characteristics of laser diodes. It has typically been considered a property of the grown material as opposed to a parameter associated with a particular device. This is evidenced in the experimental determination of the quantum efficiency from measures of external efficiency against laser cavity length. In general it represents the fraction of injected carriers that recombine radiatively and produce photons [1]. Although acknowledged to be a somewhat imprecise concept [2] it has been formulated as the ratio of radiative transitions to all transitions and expressed as [1]

$$\eta_i = \frac{Bn^2 + R_{st}N_{ph}}{A_{nr}n + Bn^2 + Cn^3 + R_{st}N_{ph}}$$

where n is the electron concentration, A_{nr} is the nonradiative coefficient, Bn^2 represents spontaneous recombination, Cn^3 is due to Auger recombination, R_{st} is the net stimulated emission rate, and N_{ph} is the intracavity photon density. This derivation of the quantum efficiency is not immediately useful in determining the value of η_i. Furthermore it is not immediately apparent how device parameters can influence the value of η_i. In this Letter the internal quantum efficiency of the laser diode is derived from the current continuity equation. The current continuity equation is written as

$$J = J_{RL} + J_{NR} + J_{DIFF} \quad (1)$$

where J_{RL} is the current due to radiative recombination (with spontaneous J_{SP} and stimulated J_{ST} contributions), J_{NR} is the nonradiative recombination comprising the recombination in the active region J_{NR1} and the recombination in the depletion regions of the diode J_{NR2}, and J_{DIFF} is the diffusion current flowing in the n and p neutral regions. These current components are illustrated in Fig. 1. The internal quantum efficiency is, in actuality, the confinement factor for electrical carriers and may be defined as the ratio of the total recombination current in the active region to the total current:

$$\eta_i = \frac{J_{NR1} + J_{RL}}{J_{NR1} + J_{NR2} + J_{RL} + J_{DIFF}} \quad (2)$$

Because η_i is determined by the ability of carriers to scatter into the active area it should be constant, independent of the injection level. Therefore its value can be determined by conditions at threshold because then J_{RL} reduces to J_{SPT}, the spontaneous contribution. Furthermore it has been shown [3] that all of the various current components at threshold may be expressed in terms of the quasi-Fermi levels. In addition the diode voltage can be expressed in terms of the quasi-Fermi level separation. Knowledge of the junction voltage uniquely determines the value of the diffusion and nonradiative recombination currents. Hence at threshold, eqn. 2 is expressed as

$$\eta_i = \frac{J_{NR1T} + J_{SPT}}{J_{NR1T} + J_{NR2T} + J_{DIFFT} + J_{SPT}} \quad (3)$$

where each component is uniquely specified by the quasi-Fermi level at threshold obtained by using the stimulated lifetime approach to laser operation [3]. Above threshold the diffusion J_{DIFF} and recombination outside the active area, J_{NR2}, continue to increase because they are supplied by the component $(J - J_{TH})(1 - \eta_i)$. This relation can be used to determine the voltage as a function of optical power [4].

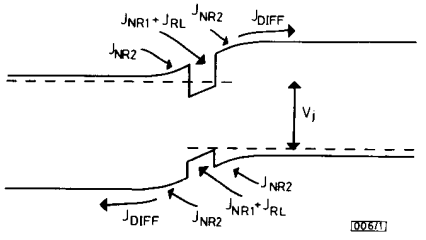

Fig. 1 *Energy band diagram and current components of laser diode under bias*

Using this formulation of the internal quantum efficiency it is possible to determine the variation in η_i with length. As the length of the laser is decreased the laser loss is increased and the Fermi level in the active region increases such that the diode voltage at threshold increases. This has the effect of increasing the relative sizes of the components J_{NR2} and J_{DIFF} resulting in a reduced value of η_i. Fig. 2 shows the internal quantum efficiency against cavity length as obtained by calcu-

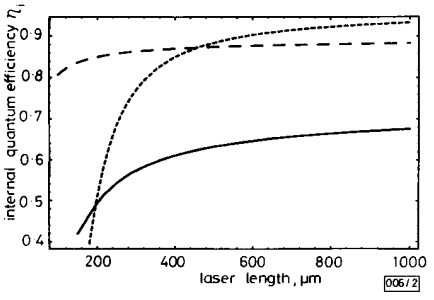

Fig. 2 *Variation of internal efficiency η_i with cavity length for SQW GaAs/AlGaAs laser, (with $\Gamma = 0{\cdot}03$, $L_z = 100$ Å, 40% Al in waveguide layers), MQW GaAs/AlGaAs laser (3 wells, $\Gamma = 0{\cdot}09$, and $L_z = 100$ Å) and strained SQW InGaAs/AlGaAs laser with $\Gamma = 0{\cdot}024$, $L_z = 80$ Å, 20% In all at $T = 300$ K*

------- SQW InGaAs
——— SQW GaAs
- - - - MQW GaAs